NON-AUTOCLAVE PROCESSING OF SANDWICH STRUCTURES: THE ROLE OF PREPREG THROUGH THICKNESS AIR PERMEABILITY

S. Sequeira Tavares, N. Caillet-Bois, V. Michaud and J.-A.E. Månson
Ecole Polytechnique Fédérale de Lausanne - EPFL
Laboratoire de Technologie des Composites et Polymères - LTC
CH-1015 Lausanne, Switzerland

Keywords: *honeycomb sandwich, air permeability, non-autoclave*

Abstract

Non-autoclave processing of honeycomb sandwich structures generally leads to poor compaction and high porosity of the skins along with a decreased skin-core adhesion. Air permeability of the skins, a critical parameter of low pressure processing, is often increased by perforating the prepregs in a patterned way, before curing of the second skin. This procedure, frequently designated as "spiking", provides an air path for the honeycomb cells voiding.

Prepreg through thickness air permeability was characterised at room temperature and its evolution monitored during cure. Several spiking configurations were tested and their role on skin-core adhesion and skin quality was evaluated. Prepreg air permeability controls skin-core bonding through the pressure drop in the honeycomb cells and potential outgassing of the adhesive layer. An optimal range of skin permeability was found to be between 5×10^{-14} cm^2 and 3×10^{-12} cm^2, which corresponds to a range of 200-600 mbar of air pressure in the honeycomb.

1 Introduction

Non-autoclave or vacuum-bag only processing of sandwich structures faces particular challenges that have no echo in the aeronautical sandwich fabrication, a consequence of only using the atmospheric pressure for their manufacturing. In particular, the adhesion of the skin to the honeycomb core is reduced, as well as the compaction of the prepreg plies within the skins. The combination of a less performing adhesion with the remaining air volume inside the honeycomb cells exposes the sandwich structure to pressure or temperature variations. Furthermore, the skins tend to have higher values of porosity, known for reducing the mechanical properties of composites, namely the compression strength and the interlaminar shear strength. On the other hand, autoclave processing is expensive, in particular for large structures, and a growing interest has been observed for vacuum-bag only processing of sandwich structures.

One way of adapting non-autoclave processing to the manufacturing of honeycomb sandwich with prepreg skins is to voluntary increase the air permeability of the prepreg. This is achieved by perforating the prepregs with a sharp tool in a patterned way. Despite this procedure, designated as spiking, the adhesion between the skin and core of a sandwich structure fabricated through vacuum-only remains less performing than for the autoclaved structures [1].

Prepreg air permeability studies have been entailed, and though starting in a rather enthusiastic way, no references on this topic are found in the last ten years [2], even though industry has approved and introduced the acquired knowledge [3]. Prepreg air permeability was mainly studied in the in-plane direction [2, 4, 5]. However, through thickness air permeation could provide new understanding to non-autoclave processing, in particular in view of honeycomb sandwich composites.

The objective of this study was to measure the intrinsic through thickness air permeability of prepregs at room temperature, as well as its evolution during the curing cycle, in processing conditions. Also, the impact of spiking on the prepreg air permeability was estimated. Mode I delamination energy G_{IC} and skin quality were then correlated to the evolution of air permeability.

2 Prepreg Air Permeability and Spiking

Figure 1 depicts observed ways of varying prepreg air permeability through spiking, i.e.,

voluntary perforation of the prepregs with a sharp tool.

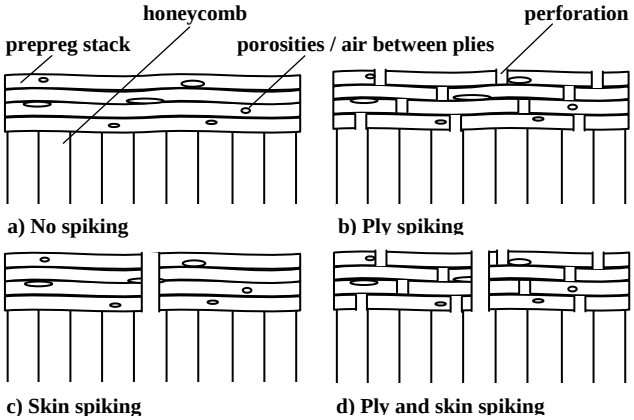

Fig. 1. Ways of varying prepreg air permeability

In particular, two types of spiking were observed in the industry. One is herein referred to as 'ply traversing' or 'ply spiking' since it is performed individually in each ply. As a consequence, when plies are stacked together the perforations do not necessarily match, as exemplified in Figure 1 b) and the air path is sinuous. The other type, referred as 'skin traversing' or 'skin spiking' is carried out once the plies are placed over the honeycomb and gives a direct passage for the air to evacuate the honeycomb cells, see Figure 1 c).

Both types of spiking have been observed in the industry, either separately or combined. Ply and skin spiking may differ in array spacing and diameter of perforation.

3 Permeability Model

Ahn et al. [6] developed an experimental method for in-plane prepreg air permeability and a model for its prediction based on Darcy's law. Method and model were further refined and air permeability was studied as a function of orientation and prepreg aging time [4]. The principle on which both model and experiment are based can be designated as a falling-pressure method and an equivalent model was derived recently for the study of asphalt air permeation [7]. The falling-pressure method requires an exchange of air imposed by a pressure differential between two volumes having as separation medium the material of which the air permeation is to be determined. In one side of the medium the pressure must be constant and the volume may be unknown. For practical reasons one can set up the experiment so that atmospheric pressure is on this side of the medium. The other side of the medium is connected to a known volume, leak free, inside which an initial pressure is imposed, typically by a vacuum pump. In view of the exclusive determination of longitudinal or transverse air permeability, it is very important to prevent air from flowing in one of the directions, which always implies some sort of sealing.

The air permeability can be calculated by monitoring the pressure variation on the confined volume until both sides are in equilibrium. The boundary conditions are the constant pressure on one side and the initial pressure on the other. For the particular case where the constant pressure is equivalent to atmospheric, the model is expressed by equation (1), where P_a is the atmospheric pressure, P_i is the initial pressure imposed in the volume V, P is the pressure at any instant t, K is the permeability, A is the area exposed to air exchange, L is the length air has to traverse and μ is the air viscosity. The air permeability can be determined from the slope of the plot of the natural log of the function on the left side of equation (1) versus time.

$$\ln\left[\frac{(P_a + P)(P_a - P_i)}{(P_a - P)(P_a + P_i)}\right] = \frac{KAP_a}{\mu LV}t \qquad (1)$$

4 Experimental Set-up

In view of a comprehensive air permeability characterization, both the intrinsic permeability and the permeability in curing conditions were determined. By intrinsic permeability is meant the permeability of the prepreg only, i.e., without vacuum-bag or any consumables. The permeability in processing conditions implies not only the use of the vacuum-bag and consumables, but also that vacuum is applied on the same side of the skin, as when performing a sandwich cure.

Both types of permeability were determined at room temperature and during the curing cycle. The air viscosity is function of the temperature, as expressed by equation (2), where μ is the viscosity and T is the temperature. This correction was introduced in the permeability model whenever necessary.

$$\mu = 4.74 \cdot 10^{-8} \cdot T + 4.17 \cdot 10^{-6} \qquad (2)$$

In order to determine the through thickness prepreg air permeability a dedicated leak tight tool was developed. It can also be used as a mould for sandwich samples fabrication in order to correlate

air permeability and final sandwich quality. The prepreg stack, sustained by a honeycomb, was placed over a cavity, see Figure 2. The prepreg was from Advanced Composites Group Limited (ACG), resin system VTM 264 34 wt% and Zoltek carbon fiber, Panex 35, unidirectional, 160 g/m^2. The prepregs were placed over an aluminum honeycomb of 3 cm height, approximately 0.4 cm of cell width and a density of 1785 g/m^2, with a stacking sequence of $[0_2/90_2]_S$. Ply sequence was symmetric with respect to the neutral axis of the skin in view of the Double Cantilever Beam (DCB) tests, carried out to determine fracture energy in delamination Mode I. When applicable, the prepreg stack was combined with a supported adhesive film from AGC, nylon support, resin system VTA 260, 313 g/m^2.

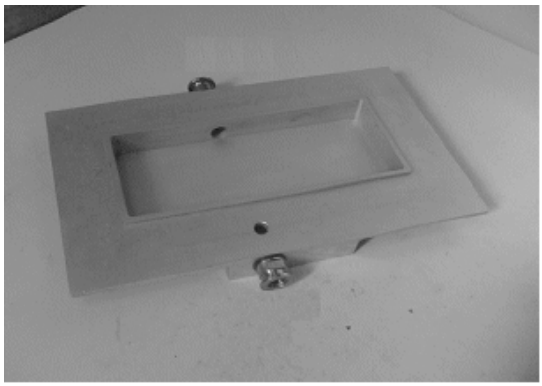

Fig. 2. Mould for the permeability measurements

The prepregs were oversized compared to the honeycomb in order to accommodate a sealant between the first prepreg layer and the metallic tool, so that air was forced to pass across the prepreg stack in the through thickness direction. Also, polyimide tape was used to seal the edges of the skin, as depicted in Figure 3.

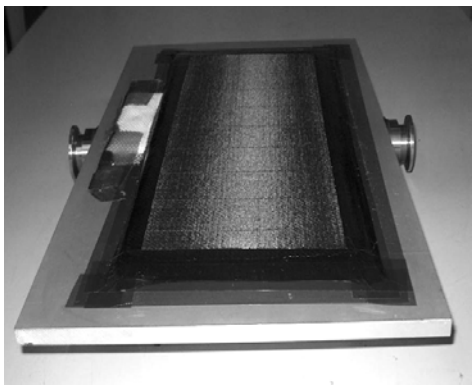

Fig. 3. Mould after sample preparation

In order to simulate the spiking types actually carried out by the industry, plates were prepared with ply spiking and combination of ply and skin spiking. Also, plates without spiking were prepared for comparison purposes. At least two plates were prepared per type of spiking. Ply spiking was performed in each prepreg layer individually with a needle of 0.8 mm diameter with an average distance of 1.3 cm between perforations. Skin spiking was performed with a needle of 2.0 mm diameter over the four prepreg plies and honeycomb core, following a squared pattern with 40 mm of distance between perforations. An extra sample was produced in which only the adhesive layer was spiked, with ply spiking.

When applicable, consumables were disposed above the prepreg stack in the following order: peelply, perforated film, absorber, breather and vacuum-bag enclosing the ensemble with a sealant against the metallic tool. For the curing of the composite samples the mould was placed inside a furnace (Heraeus UT 6200). Two curing cycles were performed. One is designated as “short cycle” and comprises a dwell of 4 h at 80 °C. The other cycle is designated as “long cycle” and includes two dwells, an initial one of 2 h at 65 °C followed by 4 h at 80 °C. In both cycles, the heating and cooling rate was of 0.5 C/min. A primary vacuum pump connected to the experiment extracted air during the measurements. The pressure inside the volume isolated by the prepreg layers and enclosing the honeycomb was recorded during cure, as well as the temperature, using a LABView interface. When applicable, the pressure inside the vacuum-bag was also recorded. The pressure sensors were from Leybold, measurement range from 1 mbar to 2000 mbar and from 5×10^{-5} mbar to 1000 mbar, respectively.

4.1 Intrinsic Air Permeability

The intrinsic permeability was determined using the model expressed by equation (1), and the experimental set-up schematized in Figure 4. V corresponds to the volume of the cavity enclosing the honeycomb, L is the skin thickness and is measured on each sample individually and A is the open area determined by the mould.

The vacuum pump extracted air from the volume enclosing the honeycomb. When an initial pressure P_i was established the vacuum pump was turned off. The pressure inside the honeycomb increased as the air flowed inside the mould through the prepreg stack. If enough time was given, the pressure would reach the atmospheric value.

However, this is not mandatory for the air permeability determination and the vacuum pump may be turned on after the pressure inside the honeycomb has increased of about 200 mbar. This procedure was repeated several times during the curing cycle and a plot of pressure versus time was obtained. Figure 5 schematically represents the pressure curve obtained during the measurements of the intrinsic permeability.

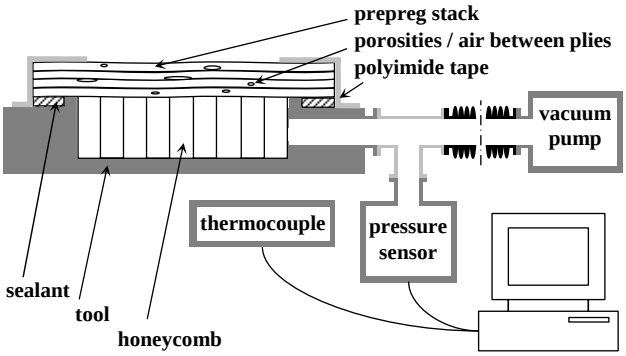

Fig. 4. Experimental set-up for measuring the intrinsic through thickness air permeability of the prepregs

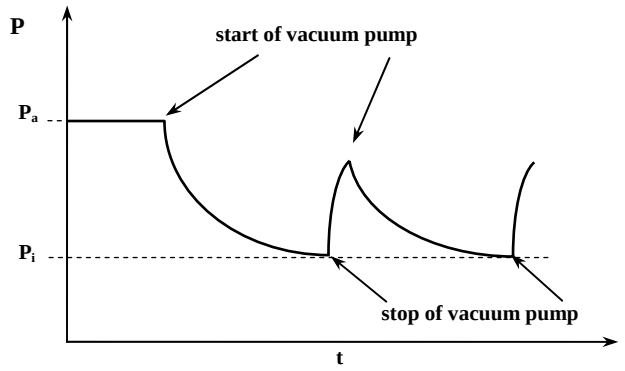

Fig. 5. Pressure curve obtained during the measurement of the intrinsic air permeability

4.2 Air Permeability in Processing Conditions

The air permeability in processing conditions was determined by using an adaptation of the experimental set-up described in the previous sub-section. In fact, the side where a constant pressure must be imposed was no longer at atmospheric pressure, but at the pressure set by the vacuum pump. This side corresponded to the side of vacuum-bag and consumables and was connected to a pressure sensor designated as “pressure sensor 2”. “Pressure sensor 1” was connected to the honeycomb side, as well as a valve, which controlled the entry of air inside the cavity where the honeycomb was enclosed. This entry of air was necessary to proceed with consecutive measurements of air permeability. The experimental set-up is schematically represented in Figure 6.

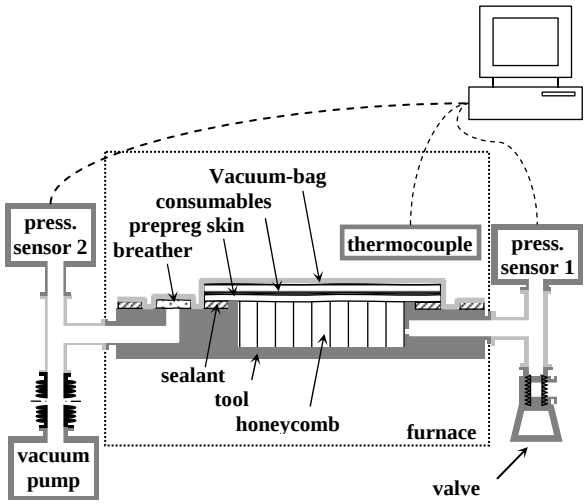

Fig. 6. Experimental set-up for through thickness air permeability measurements during cure in processing conditions

When the vacuum pump was turned on, the pressure on the vacuum-bag side decreased from atmospheric to a few mbar. Simultaneously, the pressure inside the honeycomb decreased until reaching a fairly stable value, but at a rate which depended on the skin through thickness air permeability. This procedure resulted in a set of values of pressure, allowing the determination of one value of permeability. In order to proceed with another set of values of pressure, it was needed to create again a pressure differential that led to a consistent flow of air through the skin. Therefore, the valve was slightly opened and the pressure inside the honeycomb suddenly increased. As soon as an increase in pressure of approximately 200 mbar was observed the valve was closed and the new set of values obtained. However, it was experimentally observed to be quite difficult to control the air entry by opening the valve while the vacuum pump was turned on. This was due to the imposed air drift provoked by the vacuum pump and working opposite to the opening of the valve. Therefore, the vacuum pump was turned off immediately before opening the valve and turned on as soon the valve was closed.

The model takes now the form of equation (3). The subscript on the pressure values refers to the pressure sensor registering the information. The

vacuum-bag side should ideally be at a constant pressure. Considering that the pressure variation is quite small, an average is done across the effective time range. This value corresponds to $\overline{P}_2$. The initial pressure inside the honeycomb corresponds to $P_{1,i}$ and P_1 are the values of pressure inside the honeycomb at any instant *t*. Note that the slope of the curve is now negative.

$$\ln\left[\frac{\left(\overline{P}_2 + P_{1,i}\right)\cdot\left(\overline{P}_2 - P_1\right)}{\left(\overline{P}_2 - P_{1,i}\right)\cdot\left(\overline{P}_2 + P_1\right)}\right] = -\frac{KA\overline{P}_2}{LV\mu}\cdot t \qquad (3)$$

Figure 7 represents schematically the pressure curves obtained during the measurements of the air permeability in processing conditions for "pressure sensor 1" and "pressure sensor 2". The meaning of $\overline{P}_2$, $P_{1,i}$ and P_1 is also illustrated.

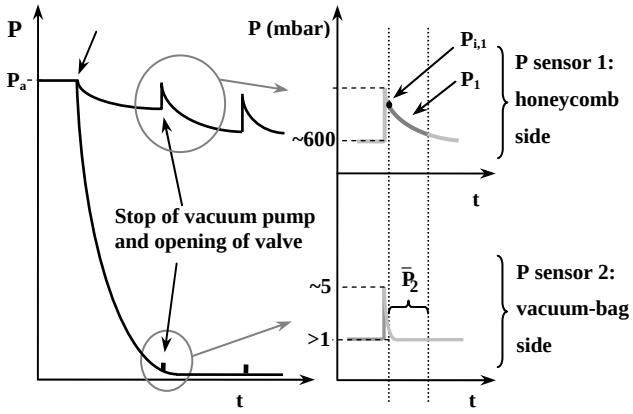

Fig. 7. Pressure curve obtained during the measurement of the air permeability during processing conditions

5 Results

5.1 Intrinsic Air Permeability

The intrinsic air permeability was determined for the prepreg stack of $[0_2/90_2]_S$ without spiking and without adhesive layer. The evolution of the permeability with cure was determined with the short cycle. The results for the prepreg stack alone are summarized in Figure 8. For better interpretation, the evolution of the resin viscosity is plotted together. As there was no vacuum-bag, i.e., no forced compaction of the plies, two types of plates were produced: one plate without pre-compaction and one plate where a pre-compaction was performed during 10 min, prior to the measurements.

Despite the different initial compactions, both plates have similar initial through thickness air permeabilities, of approximately 10^{-12} cm^2. The plate without pre-compaction had slightly lower values of permeability throughout the cure cycle. This is expected since compaction will reduce the air passages. On the other hand, these are values of out-of-plane air permeability, which should not be much affected by compaction of the plies, as for example, longitudinal air permeability would be. The curves, therefore, are in the same order of magnitude. Furthermore, the evolution of permeability during cure is quite similar, which indicates a good reproducibility of the measurements.

The evolution of the permeability follows the evolution of viscosity. The initial ramp in temperature seems to provoke a small decrease in the permeability. This may be related to an improved fiber impregnation, and, as a consequence, closure of some air passages. However, the most striking feature of the graph is the increase of the air permeability with the dramatic increase in resin viscosity. A possible explanation for this fact can be the curing of the resin itself. Although the resin is formulated to avoid shrinkage, there is always some percentage of matrix contraction, even if infinitesimal, which could open some air passages, or microcracking.

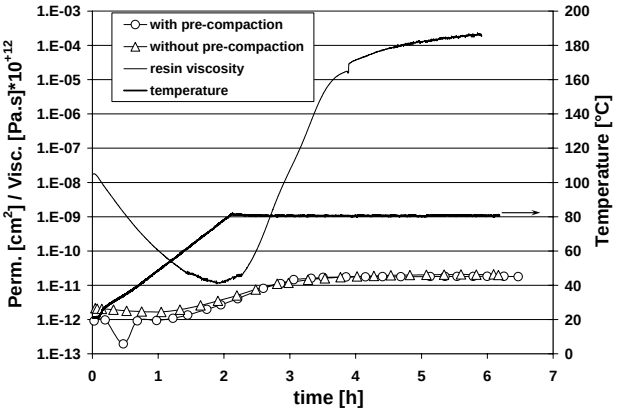

Fig. 8. Evolution of intrinsic permeability during curing of the prepreg stack alone. One plate was pre-compacted prior to the measurements

5.2 Air Permeability in Processing Conditions

The evolution of the air permeability was measured during both the short cycle and the long cycle. The short cycle was performed to set-up the process and further measurements were carried out with the long cycle.

5.2.1 Short Cycle

Two series of plates were produced with the short cycle: one series without adhesive layer, i.e., the prepregs were in direct contact with the honeycomb, and one series with adhesive layer. Two types of plates were tested in each series, plates without spiking and plates with ply spiking. Figure 9 a) and b) summarizes the results for the series without adhesive layer and with adhesive layer, respectively. The same relation between air permeability and resin viscosity, as described previously for the intrinsic permeability, occurs in both series. The values of permeability within each series are quite comparable, i.e., ply spiking is not changing the through thickness air permeability in a noticeable way.

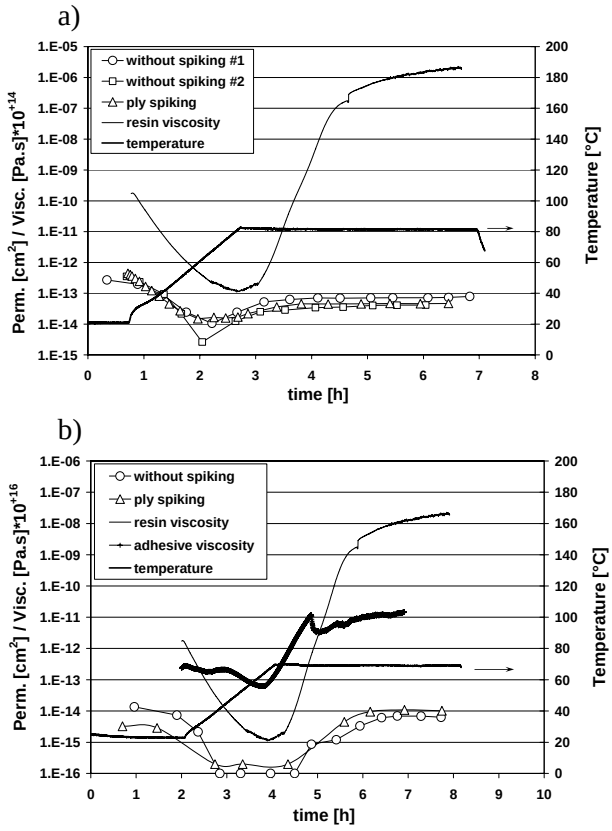

Fig. 9 Through thickness air permeability during cure with short cycle: a) without adhesive layer; b) with adhesive layer

Comparing the initial permeabilities of the samples without adhesive layer and with adhesive layer, i.e., prior to the curing cycle, a difference of about two orders of magnitude is observed. The plates without adhesive layer have an approximate initial air permeability of 3×10^{-13} cm^2 whereas the plates with adhesive layer have an initial air permeability of about 8×10^{-15} cm^2. Hence, it can be concluded that the adhesive layer is much more impermeable to air than the prepregs. Comparing the initial permeability of the series without adhesive, 3×10^{-13} cm^2, with the value of the intrinsic permeability of the prepregs, 10^{-12} cm^2, the first one is one order of magnitude lower, resulting from the air constriction caused by the various consumables.

5.2.2 Long Cycle

The results of air permeability measurements in processing conditions were obtained from plates with adhesive layer and are summarized in Figure 10. Comparing the air permeability values at the beginning of the cycle, several trends are observed. In this series of results the plate without spiking has the lowest permeability, which means that spiking can indeed modify the permeability of the skins. This fact was not observed in the results discussed in the sections above. As ply spiking is performed separately on each ply, occasionally the perforations may be in phase or closer to each other. Therefore, performing ply spiking on the prepregs may increase the skin permeability with respect to no spiking. The values lie however in the same range. Secondly, the permeability of the plate where only the adhesive layer was perforated with ply spiking – i.e., any kind of prepreg spiking was excluded – is nearly one order of magnitude higher than that of the plate with ply spiking and almost two orders of magnitude higher than that of the plate without spiking. This fact confirms that the adhesive layer is quite impermeable to air and spiking it provides a substantial impact on the skin air permeability, larger than ply spiking of the prepregs.

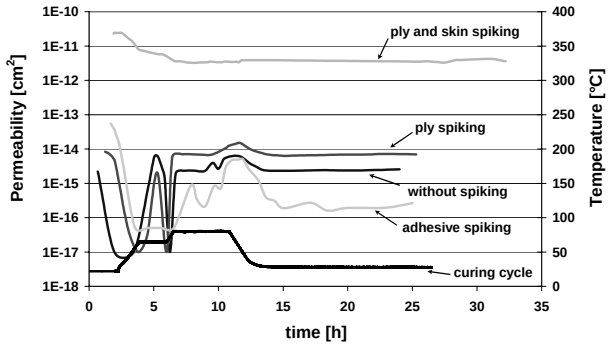

Fig. 10 Summary of the through thickness air permeability measurements

Finally, the combination of ply and skin spiking leads to the highest air permeability, of about four orders of magnitude higher than that of

the skin without spiking. This result is expected since with skin spiking the whole thickness is perforated and there is a direct passage to air. However, these perforations still imply some constriction to air passage and the permeability is still measurable.

Table 1 summarizes the equilibrium values measured before the curing cycle for the pressure inside the honeycomb and the through thickness air permeability in processing conditions, per type of spiking.

Table 1. Pressure inside the honeycomb and through thickness air permeability in processing conditions, values measured before curing cycle

Type of spiking	Initial pressure inside honeycomb [mbar]	Initial skin permeability [cm^2]
without	~ 900	~ 2×10^{-15}
ply	~ 750	~ 8×10^{-15}
adhesive only	~ 600	~ 5×10^{-14}
ply and skin	~10	~ 2×10^{-11}

5.3 Skin-core Adhesion and Quality of the Skins

From the plates manufactured with the long cycle, i.e., the ones for the study of the air permeability in processing conditions, micrographic samples were prepared as well as DCB samples. Further plates were produced to increase statistics of the DCB results. They were cured excluding any permeability measurement during cure. Plates with skin spiking were also manufactured for comparison. Their initial permeability was of about 3×10^{-12} cm^2 and the average pressure inside the honeycomb was approximately 50 mbar. These initial values are important to analyze the results of skin-core adhesion and quality of the skins since most of the ply compaction and resin flow occurs before extensive reticulation of the resin. The results will be presented in terms of pressure inside the honeycomb before cure, as this represents a more intuitive value. Nevertheless, the initials values of through thickness air permeability and pressure inside the honeycomb and inversely related: skins with higher values of through thickness air permeability induce lower values of pressure inside the honeycomb. Skin-core adhesion will be presented through the results of menisci proportions, skin-core distance and fracture energy in delamination Mode I. The width and height of the menisci were measured as depicted in Figure 11, where *w* is the width and *h* is the height. The quality of the skins was evaluated through the porosity content.

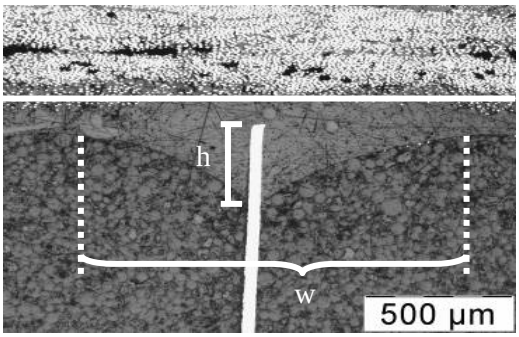

Fig. 11 Height and width of the menisci

Figure 12 summarizes the results of menisci width and height per type of spiking. Below the spiking type are indicated the equilibrium values of air permeability before cure and corresponding pressure inside the honeycomb, respectively. The width is approximately the same for all types of spiking. On the other hand, an increase in menisci height is observed with decrease of honeycomb pressure.

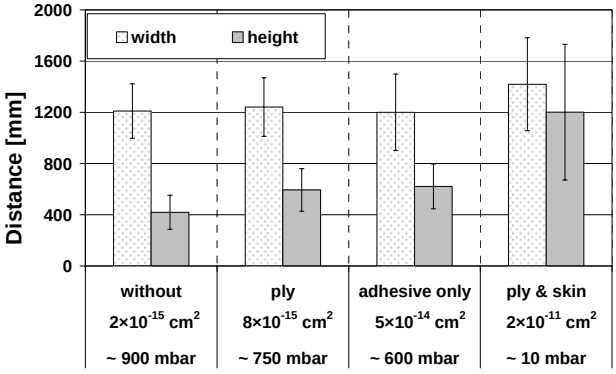

Fig. 12. Plates produced with long cycle: menisci width and height

The distance between the skin and core is plotted in Figure 13. The values decrease with decreasing pressure inside honeycomb. This reflects the pressing of the skin against the honeycomb and, logically, the lower the pressure, the more important the effect will be.

A global view of the skin-core distance and menisci height is shown in Figure 14, since their cumulative value represents the total height of the menisci, i.e., from the skin to their extremity on the honeycomb wall (see Figure 11). Although the skin-core distance decreases with decreasing pressure, the total menisci height increases.

Figure 15 summarizes the values of fracture energy in delamination Mode I obtained for all types of spiking, including skin spiking. The plate with only ply spiking of the adhesive achieves the highest value of G_{IC}. In effect, the G_{IC} values increase with decreasing honeycomb pressure until reaching the peak value for the plate with spiking of the adhesive. Afterwards, the G_{IC} values decrease with decreasing honeycomb pressure.

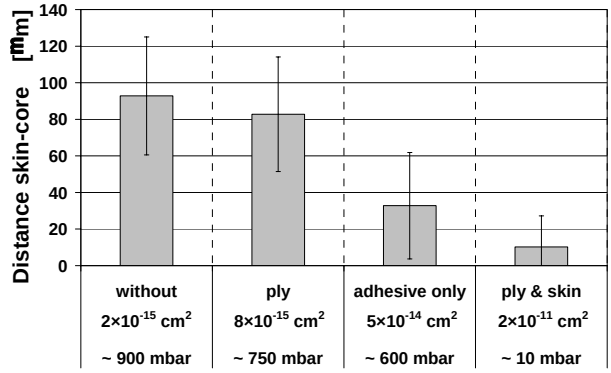

Fig. 13. Plates produced with long cycle: distance between skin and core

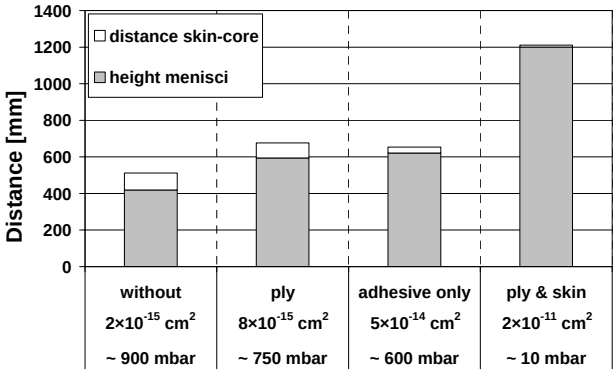

Fig. 14. Plates produced with long cycle: cumulative values of skin-core distance and menisci height

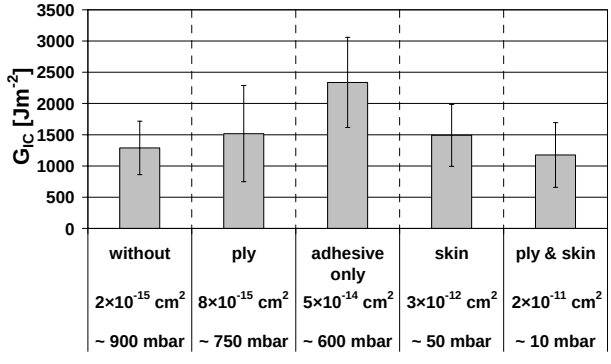

Fig. 15. Plates produced with long cycle: fracture energy in delamination Mode I.

6 Discussion of Results

6.1 Through Thickness Air Permeability

In order to analyze the evolution of air permeability in processing conditions it is interesting to plot the permeability values together with the evolution of resin and adhesive viscosity during curing. Figure 16 shows the air permeability during cure of the plates with no spiking, ply spiking and adhesive spiking.

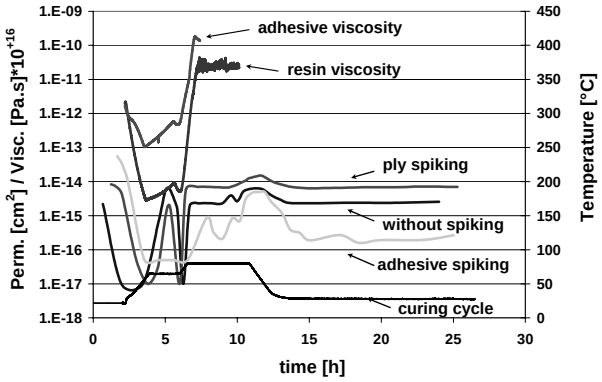

Fig. 16 Through thickness air permeability during cure with the long cycle of the plates with no spiking, ply spiking and adhesive spiking

The permeabilities of these three plates follow quite well the behavior of both resin and adhesive viscosities: during the first ramp, while viscosity is dropping significantly, the permeability is also being reduced. This is probably due to a homogenization of the adhesive film combined with an improved fiber impregnation, already referred to for the intrinsic permeability measurements. Resin flows over the small air passages, either intrinsic or made by ply spiking, therefore reducing the air permeability. During the first dwell the viscosity increases and a large raise in permeability is observed. As mentioned previously, this may be due to resin shrinkage, which could create very small air passages or to microcracking. During the second ramp in temperature, both viscosities slightly drop off and again the permeabilities follow. At the beginning of the second dwell the reticulation process is reaching a higher state and both viscosities increase dramatically, after which the matrix structure can be considered set. An increase in permeability is observed, again likely to have its origin in matrix shrinkage. During the cooling ramp there is generally a peak in permeability. The reason for this effect is still not confirmed but could be due

to a small leak provoked by differences in contraction of the mould, polyimide tape, sealant and the plate itself.

The curve of air permeability relative to the plate with ply and skin spiking shows quite different behavior with respect to the curves previously analyzed, see Figure 17. First, the permeability is almost three orders of magnitude higher than for any other type of plate, and throughout all the cycle. Second, although some variations do occur parallel to the evolution in resin and adhesive viscosities, they are not as marked as for the other plates. Although the permeability is decreasing until the viscosities of resin and adhesive increase dramatically, i.e., until the beginning of the second dwell, a subtlety can be observed with respect to the rate with which the permeability decreases. In fact, when resin and adhesive viscosities are decreasing this rate is higher and the slope of the curve increases. On the other hand, when the viscosities increase, the decreasing rate of permeability is lower. This relationship is very clear on the first heating ramp as well as on the first dwell. The fact that the relation between permeability and viscosities is more subtle when compared to the previous plates can be understood by taking into account the size of the perforations done with skin spiking. Their diameter more than doubles the one of ply spiking and even if resin is more fluid, it is not enough to close the perforations.

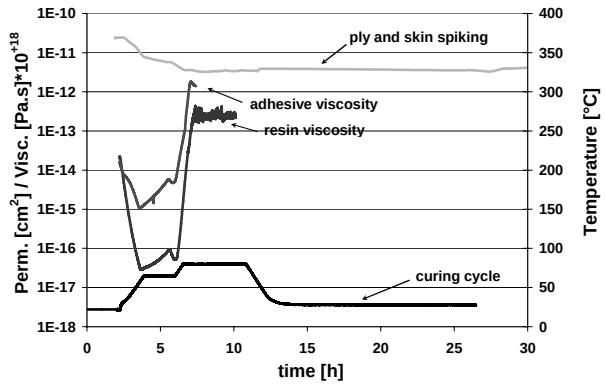

Fig. 17 Through thickness air permeability during cure of the plate with ply and skin spiking

6.2 Skin-core Adhesion and Quality of the Skins

A possible explanation for the inversion of the G_{IC} trend observed in Figure 15 lies on the adhesive degassing when the pressure inside the honeycomb is below 100 mbar. In fact, the adhesive layer for the series without spiking or with ply spiking only shows very seldom porosities, see Figure 18 a). However, the series with skin spiking, either alone or combined with ply spiking often presents large porosities, particularly at the menisci, see Figure 18 b).

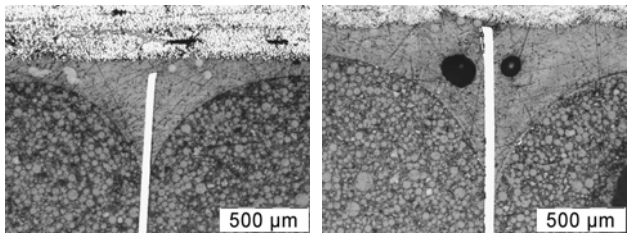

a) b)

Fig. 18. Detail of menisci from: a) ply spiking; b) ply and skin spiking

Figure 19 shows the fracture surface of the DCB samples per type of spiking. Two trends are remarked: on one hand, the width of menisci is increasing at the fracture plane with decreasing pressure. Since the width of the menisci was roughly independent from the type of spiking, the height of fracture plane changes with the honeycomb pressure, i.e., with decreasing pressure the fracture plane approaches the first ply of prepreg. On the other hand, the adhesive porosity increases with the decrease of honeycomb pressure and the adhesive layer of the plate with ply and skin spiking shows very large porosities. Therefore, there seems to be a compromise between menisci growth and adhesive degassing for which an optimal value of honeycomb pressure should be encountered. This value seems to be in the range of 200 mbar to 600 mbar, or, in terms of through thickness air permeability, between 5×10^{-14} cm^2 and 3×10^{-12} cm^2.

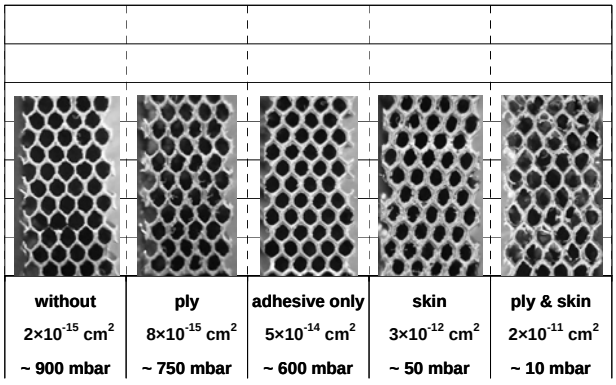

Fig. 19. Fracture surface of DCB samples after testing

The quality of the skins was accessed through the porosity content. Figure 20 summarizes the values obtained. The lowest porosity content as well

as the lowest dispersion of values are found on the series with ply spiking. The series with ply and skin spiking shows the opposite trend.

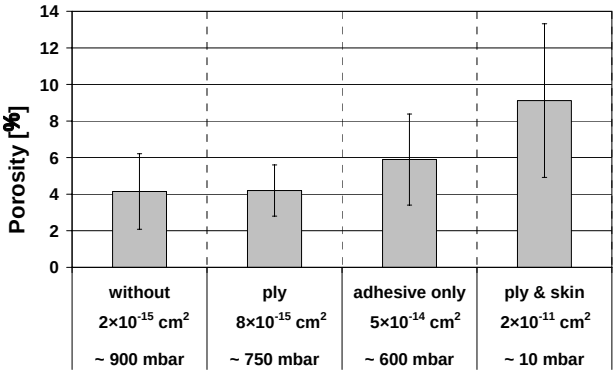

Fig. 20. Plates produced with long cycle: porosity of the skin

7 Conclusions

An experimental set-up was successfully developed and tested for through thickness air permeability measurements of skins of honeycomb sandwich structures.

The combination of ply and skin spiking results in high through thickness air permeability. Ply spiking increases slightly the permeability compared to no spiking at all.

Ply spiking contributes to improve skin quality by reducing porosity content. Skin spiking, on the contrary, increases skin porosity, resulting in higher values than for the series without spiking.

The adhesive layer was identified as the element most preventing the through thickness air permeability. The plate with spiking of the adhesive shows intermediary results of porosity content. However, taking into account the high values of fracture energy in delamination Mode I obtained for this series, it could represent a good manufacturing compromise. This suggests that in order to increase efficiently the through thickness air permeability the permeability of the adhesive layer should be changed.

Acknowledgements

This work is supported by the Swiss National Science Foundation, under project n° 200020-105169. Décision S.A. is acknowledged for fruitful discussions.

References

[1] Bonjour F., Amacher R., Michaud V., Cardis B., and Månson J.-A.E. "Vacuum-bag processing of large composite structures for America's Cup class boats". *Proceedings of The 24th International Conference and Forum - SAMPE Europe Conference*, Paris, pp 507-513, 2003.

[2] Shim S.B. and Seferis J.C. "Thermal and air permeation properties of a carbon fiber toughened epoxy based prepreg system". *Journal of Applied Polymer Science*, Vol. 65, No. 1, pp 5-16, 1997.

[3] Harmon B., Boyd J., and Thai B. "Advanced products designed to simplify co-cure over honeycomb core". *International SAMPE Symposium and Exhibition (Proceedings)*, Vol. 47 I, No., pp 502, 2002.

[4] Putnam J.W. and Seferis J.C. "Prepreg gas permeation as a function of fiber orientation and aging time". *Journal of Advanced Materials*, Vol. 26, No. 3, pp 35-41, 1995.

[5] Nam J.D., Seferis J.C., Kim S.W., and Lee K.J. "Gas permeation and viscoelastic deformation of prepregs in composite manufacturing processes". *Polymer Composites*, Vol. 16, No. 5, pp 370-377, 1995.

[6] Ahn K.J., Seferis J.C., Price J.O., and Berg A.J. "Permeation measurements through prepreg laminates". *Sampe Journal*, Vol. 27, No. 6, pp 19-25, 1991.

[7] Li H.L., Jiao J.J., and Luk M. "A falling-pressure method for measuring air permeability of asphalt in laboratory". *Journal Of Hydrology*, Vol. 286, No. 1-4, pp 69-77, 2004.